Water Resources Research

TECHNICAL REPORTS: METHODS
10.1029/2021WR031064

Tracking Microplastics Across the Streambed Interface: Using Laser-Induced-Fluorescence to Quantitatively Analyze Microplastic Transport in an Experimental Flume

Jan-Pascal Boos[1], Benjamin Silas Gilfedder[1,2], and Sven Frei[1]

[1]Department of Hydrology, Bayreuth Center of Ecology and Environmental Research (BAYCEER), University of Bayreuth, Bayreuth, Germany, [2]Limnological Research Station, Bayreuth Center of Ecology and Environmental Research (BAYCEER), University of Bayreuth, Bayreuth, Germany

Key Points:

- Novel methodology for the analysis of microplastic (MP) transport in a water flume
- Quantitative, spatiotemporal information of MPs through fluorometric techniques
- First direct observation of advective transport of MPs through the hyporheic zone using natural sediments

Supporting Information:

Supporting Information may be found in the online version of this article.

Correspondence to:

J.-P. Boos,
Jan-Pascal.Boos@uni-bayreuth.de

Citation:

Boos, J.-P., Gilfedder, B. S., & Frei, S. (2021). Tracking microplastics across the streambed interface: Using laser-induced-fluorescence to quantitatively analyze microplastic transport in an experimental flume. *Water Resources Research*, *57*, e2021WR031064. https://doi.org/10.1029/2021WR031064

Received 19 AUG 2021
Accepted 23 NOV 2021

Author Contributions:

Conceptualization: Benjamin Silas Gilfedder, Sven Frei
Data curation: Jan-Pascal Boos
Funding acquisition: Benjamin Silas Gilfedder, Sven Frei
Investigation: Sven Frei
Methodology: Jan-Pascal Boos, Benjamin Silas Gilfedder, Sven Frei
Project Administration: Benjamin Silas Gilfedder, Sven Frei
Software: Jan-Pascal Boos, Sven Frei
Supervision: Sven Frei
Visualization: Jan-Pascal Boos
Writing – original draft: Jan-Pascal Boos

Abstract Rivers and streams are a primary transport vector for microplastics (MPs), connecting terrestrial sources to marine environments. While previous studies indicated that pore-scale MPs can accumulate in streambed sediments, the specific MPs transport and retention mechanisms in fluvial systems remain poorly understood. As part of this technical note, we present a novel method for a quantitative analysis of the spatiotemporal transport and retention of pore-scale MPs in an experimental flume. A continuous mass balance for MPs in surface water was achieved using two online fluorometers, while a laser-induced Fluorescence-Imaging-System was developed to track and quantify the spatial migration of MPs through the streambed sediments. The detection limit was <1 µg/L for 1 µm polystyrene microbeads with the fluorometers and 3 µg/L for the Fluorescence-Imaging-System. The system was able to quantitatively track the advective transfer of MPs into the streambed sediments: a process that has yet not been observed experimentally. Results showed that MPs infiltrated into the streambed sediments up to a depth twice the bedform amplitude. This work provides a novel experimental method to quantitatively monitor MP transport through porous media and advective exchange of MP across the streambed interface.

1. Introduction

Microplastics (MPs), synthetic polymer particles smaller than 5 mm (Frias & Nash, 2019), are omnipresent in the hydrosphere (Andrady, 2011; Li et al., 2020) as well as in marine, riverine and limnic biota (Carbery et al., 2018; Jemec et al., 2016; Windsor et al., 2019). Detection of MPs in remote areas such as the deep-sea (Woodall et al., 2014), polar regions (Peeken et al., 2018) and remote lakes (Free et al., 2014) as well as their accumulation in ocean gyres (Law et al., 2010) highlight the importance of understanding transport mechanisms responsible for distributing MPs from source areas to these various environmental compartments. The majority of marine MPs is transported to the ocean by rivers and streams (Meijer et al., 2021). MPs enter stream and river systems through both point and diffuse sources including wastewater treatment plants, the atmosphere and surface runoff (Skalska et al., 2020).

The mobility and retention of MPs in fluvial systems depends on catchment properties (Baldwin et al., 2016), hydrodynamic characteristics (Haberstroh et al., 2020), physicochemical interactions (Lu, Gilfedder, Peng, Niu, & Frei, 2021; Lu, Gilfedder, Peng, Peiffer, et al., 2021) and particle properties (Waldschläger & Schüttrumpf, 2019a). MP accumulation has been observed in low flow regimes such as lakes and reservoirs (Tibbetts et al., 2018) as well as behind flow obstacles (Los Santos et al., 2021; Watkins et al., 2019) and morphological streambed features such as ripples and dunes (Mani et al., 2019), constituting either temporary or permanent retention areas (Horton & Dixon, 2018).

High numbers of MPs have been detected in surface flow, at the streambed interface and in streambed sediments (Shahul Hamid et al., 2018). Along with sedimentation, advective transfer of MPs across the streambed interface into the sediments has been discussed as a potential transport pathway for pore-scale MPs into the hyporheic zone (HZ) and shallow groundwater (Frei et al., 2019). Similar to aqueous phase contaminants (Elliott & Brooks, 1997), pore-scale MPs have also been shown to be mobile in porous media such as streambed sediments (Drummond et al., 2020) or alluvial aquifers (Goeppert & Goldscheider, 2021). Contrarily, MPs can be retained in streambed sediments due to physical clogging of pores (Nizzetto et al., 2016) or sorption effects (Lu, Gilfedder,

Writing – review & editing: Jan-Pascal Boos, Benjamin Silas Gilfedder, Sven Frei

Peng, Peiffer, et al., 2021). During flooding, previously retained MPs can be re-mobilized from the streambeds by erosion (Ockelford et al., 2020).

MP transport in rivers and streams depends on particle characteristics such as shape, size, density and surface characteristics (Kowalski et al., 2016). As the mathematical formulation of transport equations was originally developed for natural sediments, mainly mineral particles of high density and spherical shape, they are only approximately representative for MPs (Hoellein et al., 2019; Waldschläger & Schüttrumpf, 2019b). Thus, additional studies explicitly investigating the transport mechanisms of MPs in streams and rivers are required. MPs have been found to be stored more shallowly in and released more rapidly from the HZ compared to solutes in field studies (Harvey et al., 2012), highlighting the importance of hyporheic exchange for MPs smaller than 100 µm (Drummond et al., 2020). The mobility of bigger MPs (>600 µm) in porous media was previously investigated using column experiments packed with glass beads, showing that retention strongly depended on the relative particle size (Waldschläger & Schüttrumpf, 2020). However, particle migration was not continuously monitored, and results from column experiments are difficult to transfer to stream systems with pronounced three-dimensional hydrodynamical forces that are directly determined by the specific shape of bed form structures.

While MPs migration between surface flow and the HZ has been postulated (Frei et al., 2019), the detailed exchange mechanisms and the specific roles of advective transfer, erosion and sedimentation of MPs in riverine systems have not been experimentally investigated. As part of this technical note, we present an experimental setup for dynamic monitoring and quantification of pore-scale (1–10 µm) MPs abundances in (a) surface flow, (b) at the streambed interface and (c) in hyporheic sediments for an experimental flume environment. The methodology is versatile as it can be used to establish mass balances for MPs in the surface water as well as quantify the spatiotemporal dynamics of MPs in the sediments. This can be linked to the hydrodynamic conditions and bedform morphology for a deeper mechanistic understanding of the transport and retention behavior of MPs in fluvial systems.

2. Materials and Methods

2.1. Set-Up of the Experimental Flume

The experiments were carried out in a tiltable, closed-circuit flume (G.U.N.T. GmbH) with a rectangular cross-section (500 × 8.6 × 30 cm, Figure 1). The inlet water was intermittently stored in a reservoir of 250 L in which water temperature and water level was continuously monitored using a levelogger (Solinst Ltd). Deionized water was used for all experiments, which was conveyed to the flume by a centrifugal pump (Ebara S.p.A.). Discharge in the flume was adjusted between 0.5 and 2.5 Ls^{-1} using an electropneumatic valve (GF Ltd.) and monitored continuously with an electromagnetic flow meter (Jumo GmbH).

2.2. Microplastic Particles

The experiments were performed with polystyrene (PS) microbeads with a diameter of 1 and 10 µm and density of 1.05 g mL^{-1} (PolySciences Inc.). The particles have an internal fluorescent dye, characterized by an excitation maximum at 441 nm and emission maximum at 486 nm. The stock particles have a concentration of 2.6% in aqueous suspension and are coated with a tenside (sodium dodecyl sulfate). An intermediate dilution was prepared by diluting 100 mg of stock solution in 50 mL deionized water. The final calibration suspensions were obtained by further dilution. Particle numbers were calculated using particle density and size and were $\sim 2 \cdot 10^6$ particles/µg. The stock suspension was kept dark and refrigerated at 4°C to avoid thermal as well as photochemical degradation. After each experiment, flume and sediments were thoroughly rinsed with deionized water to remove MPs from the system. The signal of any remaining MPs (lower than the detection limit) was incorporated into the blank signal measured in subsequent experiments. MP laden water from previous experiments was repeatedly pumped through a filter cascade of two membrane filter cartridges with mesh 0.45 µm (Fuhr GmbH), until no MPs were detected and subsequently, the water was released into the sewage system.

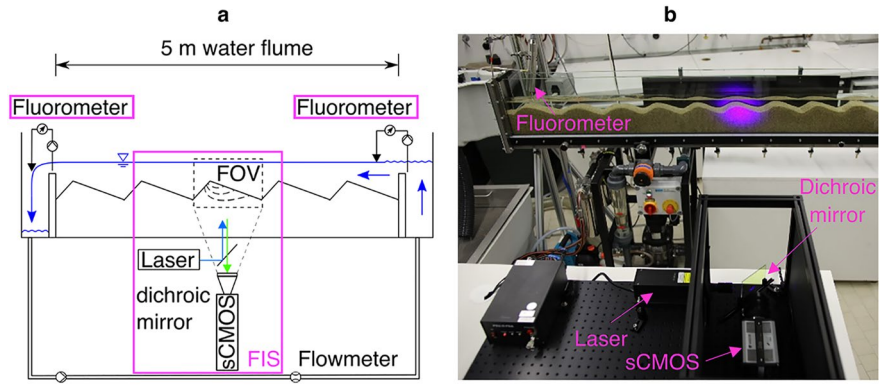

Figure 1. Schematic (a) and photo (b) of the experimental water flume setup showing the applied MPs tracking techniques: Two fluorometers at the inlet and outlet of the flume measure surface water concentrations of MPs. The Fluorescence-Imaging-System (FIS) is used to measure both surface water and pore water MP concentrations by analyzing the fluorescence signal registered by the scientific complementary metal-oxide-semiconductor (sCMOS) sensor. The camera's field of view (FOV) indicates the measurement area.

2.3. Quantification of Microplastic Transport and Retention

2.3.1. Monitoring of MPs in the Surface Water

Continuous in-situ measurement techniques were employed for real-time monitoring of MP abundances in the surface flow. The volumetric particle concentration was measured at the in- and outflow of a control volume with two portable fluorometers (FL24, Albillia Co.) which measure the MP concentration of up to three fluorophores by optical excitation and detection in a flow cell (Schnegg, 2002). Given the fluorescent properties of the MPs, the uranine channel with excitation at 470 nm was selected, using a maximum measurement frequency of 0.5 Hz. Water was extracted from the flume with a peristaltic pump, transferred through the flow cell of the measurement device and returned into the flume. Particle adhesion in the tubing was assumed negligible by choosing a material with smooth inner surface (Tygon E-3609) and minimizing tube length. In contrast to a solute, the fluorescence signal of MP particles passing through the flow cell is discrete in nature and characterized by rapid fluctuations in signal strength and intensity. Calibration of the portable fluorometers was conducted individually for the 1 and 10 µm particles to compare particle detection limits and linearity (Exp. 1 in Table S1 and Figure S1 in Supporting Information S1). Table S1 in Supporting Information S1 provides an overview of the experiments. The measurement signal was corrected by subtracting the blank signal caused by light reflection in deionized water, which was assumed to be stable throughout the experiment. Outliers were removed from the data and a mean value of approximately 30 measurements was used for each calibration standard. The concentrations were grouped in decadal intervals for regression analysis. Quantification and detection limits were calculated using the static model from the calibration curves (Tables S2–S4 in Supporting Information S1).

2.3.2. Manual Sampling of MP in Surface Water and Subsurface Water

Water samples from surface water or pore water were manually collected and analyzed using a laboratory fluorescence spectrometer (LS 55, Perkin Elmer Inc.). The samples were analyzed using a fixed wavelength that matched the peak excitation wavelength of the fluorophore of 441 nm. The emission signal was recorded between 450 and 550 nm with a resolution of 0.5 nm. The peak height at 486 nm as well as the peak area, integrated over the entire measured spectrum and a narrower wavelength interval of 460–540 nm, were used in the linear regression analysis. Triplicates of each sample were analyzed to enhance measurement precision. This method was calibrated for the 1 µm PS beads (Exp. 2).

2.3.3. Monitoring MP Transfer Across the Streambed Interface Using Laser-Induced-Fluorescence Imaging

For a single bedform structure, a scientific complementary metal-oxide-semiconductor (sCMOS) camera (Andor Zyla 5.5, Oxford Instruments) was used to measure the fluorescent signal of MPs in the (a) surface flow, (b) at the streambed interface, and (c) in the pore space of the streambed. Two diode-pumped solid state-lasers (CNI Ltd.,

$\lambda = 457$ nm) were used to excite the fluorescence dye in the MP. For full illumination of the camera sensor, the laser beam was expanded using a 2X Beam Expander (Laser 2000 GmbH). The optical path of the solid-state laser light was diverted perpendicularly to the flow, using a 45° dichroic mirror (Chroma Technology Corp) which significantly reduces the amount of excitation light from entering the detector. The fluorescence light was additionally filtered using a longpass filter (Edmund Optics Inc) mounted on the camera objective (f/0.95, 50 mm focal length) before detection by the imaging sensor (2160*2560 pixel, 6.5 µm pixel length). This Fluorescence-Imaging-System (FIS) was mounted on an optical breadboard which was positioned on a height-adjustable table.

The calibration of the FIS for surface water and porewater was conducted on a 10 cm long, isolated section of the flume filled with (a) MP suspensions and (b) MP suspensions in the pore-space of the streambed sediments (Exp. 3 in Table S1 in Supporting Information S1). The calibration area was centered in the camera's field of view (FOV) to increase measurement sensibility. The dimensions of the calibrated region, the region of interest (ROI), were 7 × 6 cm with a spatial resolution of 160 µm/Pixel. As fluorescence intensity varied over the field of view, local linear regressions were carried out for squares of 10 × 10 pixels, yielding individual calibration slopes m. To achieve a homogeneous distribution, m was additionally filtered with a 2d Gaussian filter ($\sigma = 2$). The calibration slope represents the local sensitivity of the FIS, which primarily depends on laser illumination. To account for a potential variation in average light intensity between different calibrations, the slope distribution was normalized by its average value. In the pore-water, the fluorescence signal was heterogeneously distributed caused by a non-reproducible local positioning of grain edges and pore water. Noting a linear correlation for the ROI averaged values (Figure S4 in Supporting Information S1), the calibration slope was obtained by scaling the slope distribution in surface water with the ROI-averaged slope of the pore-water calibration.

An analysis of areas larger than 7 × 6 cm required an additional calibration, which was conducted using a purpose-built glass tank of dimensions 60 × 30 × 5 cm positioned inside the flume (Exp. 4 in Table S1 in Supporting Information S1). The slope distribution in the water-filled tank was scaled by the average slope of the calibration inside the flume to obtain the final calibration relation. To ensure a reliable quantification, only areas were considered that possessed a correlation coefficient of $R^2 > 0.90$, which coincided with the highest illumination (Figure S3 in Supporting Information S1).

Before and after the experiments, reference measurements were carried out to compensate for a possible change in light illumination and to extract the position of sediment, water and air interfaces. Data acquired prior to MP input was used for background-subtraction. After binning squares of 10 × 10 pixel, the image was gaussian filtered to achieve higher illumination homogeneity in the pore-water phase. We obtained a vertical profile of MPs in the surface and subsurface water by taking vertical slices at a fixed longitudinal position, averaging the pixel-wise calculated concentrations over a given length (1 cm). The calculations were performed using the image processing toolbox in MATLAB (The MathWorks Inc., 2019).

2.3.4. System Sensitivity

To assess the reproducibility of the analytical measurement techniques, four MPs pulse injection experiments were conducted using deionized water at mean velocity of 0.08 m s^{-1} and without sediments (Exp. 5 in Table S1 in Supporting Information S1). A non-recirculating water flow was chosen to avoid masking the tail of the breakthrough curve by the arrival of recirculated water with higher MP concentrations. The instruments were calibrated prior to each experiment. The fluorometers were positioned at the in- and outflow of the flume (at 0 and 5 m respectively) and the FIS was focusing on an area of 7 × 6 cm at 3 m along the flume. An obstacle of 10 cm height was positioned at the outflow to ensure that the camera FOV was entirely filled with water. 231 µg of MPs ($\sim 4 \cdot 10^8$ particles) were injected instantaneously into the inlet of the flume, with concentrations of the suspension varying between 46 and 150 mg/L. The experiment finished when the concentration of MPs fell below the detection limit of all measurement devices (~4 min). The mass recovery was estimated by temporally integrating MPs breakthrough curves $Q \cdot \int c \ \mathrm{d}t$, assuming homogeneity in particle distribution over the cross-section of the flume.

2.3.5. Application Example: Quantification of MPs Mobility and Retention

As a proof of concept, we tested the analytical methods to quantitatively track and quantify the transport and retention behavior of MPs in the flume environment (Exp. 6 in Table S1 in Supporting Information S1). The flume was filled with a coarse sand to represent typical streambed deposits (mean diameter $d_{50} = 1.0$ mm, hydraulic conductivity $K = 3.4 \cdot 10^{-4}$ m/s, porosity $n = 0.29$). A sequence of 17 consecutive ripple bedforms with a crest

length of 15 cm, trough length of 5 cm and amplitude of 3 cm were shaped inside the flume. This geometry was based on an analytical description (Haque & Mahmood, 1985) of bed forms commonly found in streams (Fox et al., 2014) with subcritical flow and low Froude numbers (Engelund & Fredsoe, 1982). Impermeable weirs were used to ensure bedform stability and define the control volume (height 15 cm, located at 80 and 500 cm distance from the flume inlet). Water was recirculated at 0.17 m s^{-1}.

The fluorometers were centered at the weir overflows, measuring at 0.5 Hz. The frame of the FIS was centered on the streambed-water interface of the twelfth bedform (between 3.65 and 3.85 m), to avoid disturbances in the flow field caused by the weirs. The camera aperture was set to its maximum (f/0.95) to enhance light throughput. Images were recorded using an exposure time of 1 s at a frame rate of 0.5 Hz. 26 mg MP of 1 µm diameter were injected as a pulse into the surface flow at the inlet of the flume and the temporal evolution of particle flow (breakthrough) (a) in the surface flow, (b) at the streambed interface and (c) in the streambed sediments was quantitatively monitored using the methods described above.

3. Results and Discussion

3.1. Calibration, Detection, and Quantification Limits

For the two portable fluorometers, the calibration was linear in a range between 0.4 and 4,000 µg/L (lowest R^2 of 0.97, Exp.1, Figure S1a in Supporting Information S1). The detection limit was 0.6 µg/L and the quantification limit was 0.9 µg/L (Table S2 in Supporting Information S1). The fluorometers were less sensitive for the 10 µm particles (detection limit ≈ 50 µg/L) which was attributed to a decrease in particle abundance and surface area in the measurement cell (Text S4 in Supporting Information S1). However, the correlation was still linear with the lowest R^2 being 0.76. Results from the offline fluorescence spectroscopy (Perkin Elmer, Exp. 2, Figure S1b in Supporting Information S1) using the wavelength interval between 460 and 540 nm yielded high coefficients of determination (all $R^2 > 0.93$) and the lowest deviations in triplicate analysis. The detection and quantification limits were comparable to the in-situ fluorometers at 0.5 and 0.8 µg/L, respectively (Table S3 in Supporting Information S1).

For the FIS (Exp. 3), the analysis of a 7 × 6 cm isolated flume section yielded a linear correlation with a mean $R^2 > 0.99$, detection limit of 3.1 µg/L and a quantification limit of 4.7 µg/L (Figure S2 and Table S4 in Supporting Information S1). Small differences in regressions slope were observed in the triplicated calibration, although the position of the FIS was not intentionally changed. The distribution of regression slopes and regression coefficients of the calibration of the FIS for a larger FOV as needed for the infiltration experiment is shown in Figure S3 in Supporting Information S1 (Exp. 4 in Table S1 in Supporting Information S1).

All measurement techniques were characterized by linear relations with high R^2 values, thus providing reliable data for the quantitative evaluation of MPs concentrations. The methods are comparably sensitive as their detection limits are low (<3 µg/L for the 1 µm beads), which reduces the quantity of MPs needed for an individual experiment. These findings agree with previously published data on detection limits for a fluorescence spectrometer using the same 1 µm beads (Goeppert & Hoetzl, 2010).

3.2. Recovery Rate of Pulse Injection Experiments

The MP recovery rates of the Fluorometers and the FIS, acquired in three experiments with linear flow, varied between 80% and 90% (Exp. 5, Figure 2). For the Fluorometers, the MP loss is most likely due to non-uniform MP concentrations in the flume, as in pilot tests particle concentration varied somewhat in vertical and lateral sampling locations. The deviance in FIS data might be caused by the focus being on the inner flume interface: Since the velocity distribution is affected by the no-slip boundary condition located at the water-glass interface, less MP is transported near the boundary, meaning that the lateral integration of the FIS underestimates particle abundance. In addition, experiments with higher flow velocity caused by removing the outflow obstacle displayed a higher recovery rate (>95%). Missing MPs can also be attributed to the adhesion of particles to the glass sides and the bottom of the flume.

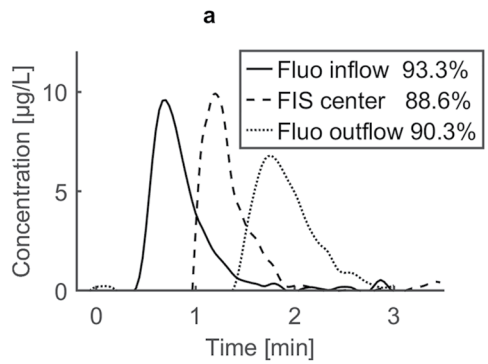

b

Run	Recovery Rates [%] Fluo inflow	FIS center	Fluo outflow
1	93.3	88.6	90.3
2	87.1	76.0	76.7
3	87.8	79.0	77.4
4	84.0	80.5	83.7
mean	**88.1**	**81.0**	**82.0**

Figure 2. Breakthrough curves of a MP pulse in the flume, with non-recirculating flow and without sediment (Exp. 5). Fluorometer are positioned at in- and outflow (0 and 5 m), the FIS at 3 m. (a) Breakthrough curves for run 1, data is interpolated with splines. (b) Results of the relation of recovered to total MP mass in four experiment runs.

3.3. Quantification of MP Mobility and Retention

In- and outflow MP concentrations of the breakthrough experiment (Exp. 6) are shown in Figure 3a. The time lag between the fluorometers was 22 s, yielding an advective transport velocity of 0.19 m s^{-1}. This agrees with a mean transport velocity of 0.17 m s^{-1}, calculated from the discharge (0.69 L s^{-1}) and the average water depths at bedform crest (26 mm) and trough (40 mm). Comparing the fluorometers, MP peak arrival was delayed by 26 s, indicating minor dispersion effects on peak transport velocity. For the outflow fluorometer the peak concentration was 33% lower (1,740 µg/L vs. 1,170 µg/L), and peak width, measured as full width at half maximum, was 67% higher than at the flume inlet (15 and 25 s). This shows that the breakthrough at the upper fluorometer was mainly influenced by advection, whereas the second measurement site was influenced by advection, dispersion, and probably retention.

The MPs concentration increased again after 99 s at the inflow and 137 s at the outflow due to water recirculation through the flume reservoir. The minimum MPs concentration was 0.1%, respectively 2.3% of peak concentration. An analysis for the recovery during the first pulse of MP yielded 72% for the inflow, and 92% for the outflow fluorometer. The low recovery was most likely caused by a heterogeneous distribution of MPs in the flow closer to the inlet. Details of the tail of the breakthrough curve cannot be evaluated since concentrations were masked by the arrival of MPs-laden recirculated water. After the initial breakthrough, monitoring with Fluorometers yielded similar concentrations of MPs at the in- and outflow of the flume. MPs concentration in the surface water decreased throughout the experiment, beginning at 118 µg/L, and ending at 103 µg/L after five hours (Figure 3a).

For the same experiment, the fluorescence-imaging-system was used to quantify the MPs concentrations in the surface flow above the bedform, at the streambed interface and in the streambed sediments. Depth specific breakthrough curves, averaged over 1 cm depth, are shown in Figure 3b. The datasets show a synchronous peak, independent of sediment depth, at the time of arrival of MP in the surface water (45 s after injection). This effect was physically implausible, given the lower hyporheic flow velocities in the porous medium, which additionally decrease with sediment depth. The effect was attributed to charge spillage (sensor blooming) caused by the oversaturation of individual pixels. The secondary peaks in the subsurface datasets indicated the migration of the MPs plume through the streambed sediments. A non-linear relation between sediment depth and peak arrival time as well as peak concentration could be noticed. Between 1 and 7 cm sediment depth, breakthrough peak time increases from 89 to 251 s, while peak concentration dropped from 630 to 180 µg/L. MPs infiltration was observed to a depth twice the bedform amplitude. After the initial breakthrough, the concentration in the individual sediment depths showed only little variation in time. The FIS data in the surface water showed a declining surface water concentration, starting at 125 µg/L and ending after four hours at 105 µg/L. The values of the FIS data set were similar to the Fluorometer surface water measurements. Figure 3c provides a timeseries of MPs infiltration and a video is available in the supplementary materials.

The application of an injection of MP into the surface water of the flume showed that our experimental setup can be used to investigate transport, exchange and retention of pore-scale MPs in the surface water as well as in the streambed sediments. MP transport in the surface water shows patterns of advection and longitudinal dispersion,

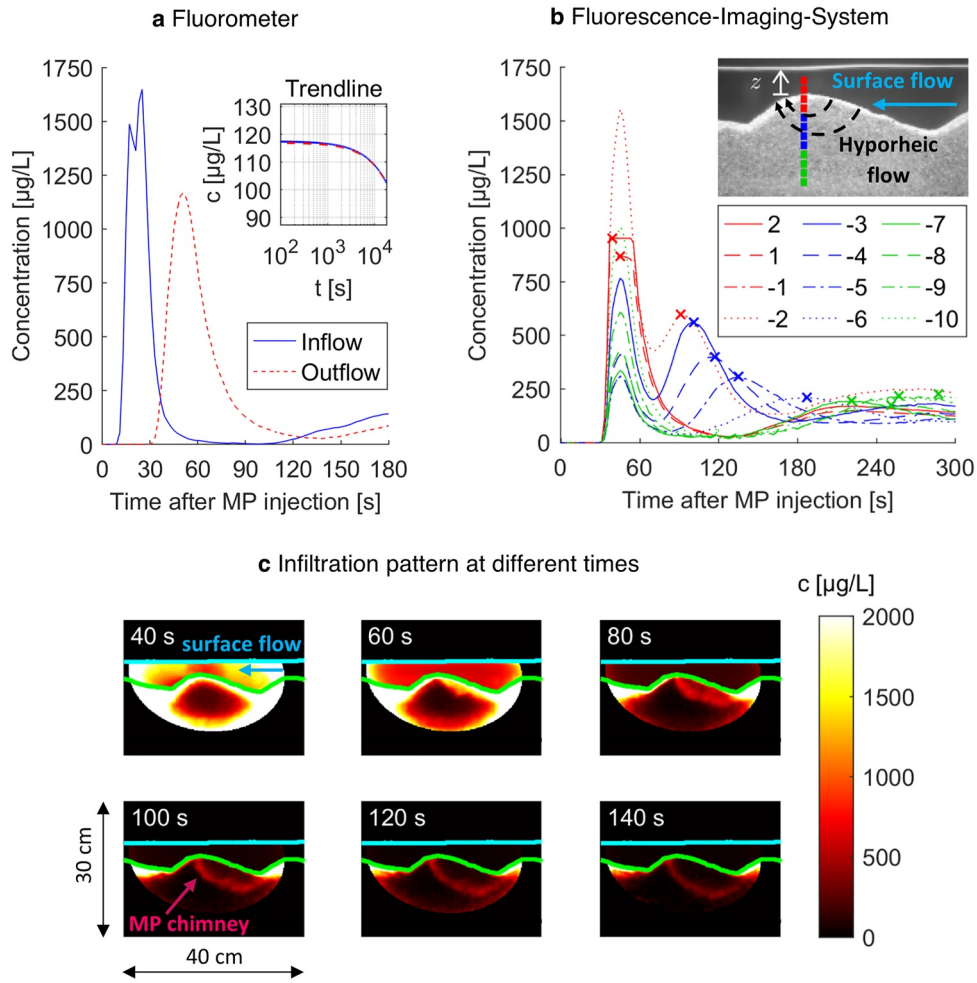

Figure 3. Microplastics (MPs) transport during infiltration experiment (Exp. 6). (a) Concentration in surface water flow at flume inflow and outflow, monitored with Fluorometers. The inset plot shows an exponential trendline. (b) Vertical profile of MPs breakthrough at the ripple crest, slice depth was 1 cm, numeration shows elevation above sediment-water-interface. Peak concentration in the surface is cut off due to over-saturation. Concentration increases after ~2 min due to recirculation. (c) Time series of MPs infiltration, captured with the FIS (air-water-interface in cyan, water-sediment-interface in green, surface flow from right to left). The camera frame is oversaturated at the arrival of MPs in surface water (at 40 s). Particle infiltration depth reaches twice the bedform amplitude. Particles reenter the surface water flow at the downstream face, preferentially in vicinity to the bedform crest.

leading to a less pronounced but lengthier breakthrough in the flume outlet, as has been already noted in previous experiments (Cook et al., 2020). With the FIS system, for the first time, we were able to directly track the advective transfer of MP particles across the streambed interface and flow through the HZ.

Peak concentrations were higher in shallow areas of the sediments. MPs concentrations in the surface water during the peak of the first breakthrough as observed by the FIS, focusing on the center of the control volume, were lower than at the outflow fluorometer. This was probably caused by the oversaturation observed in the FIS. After the first breakthrough, the datasets yielded comparable surface water concentrations (Figure 3a, inset). However, while demonstrating MP infiltration into the streambed sediments, the current data set gives no clear indication on whether particles in the hyporheic zone are immobilized after the first breakthrough or are transported conservatively with the advective flow. Additionally, the surface water concentration continuously decreased during the timescale of the experiment (5 hr). Although this was partially attributed to deposition in the flume apparatus, it is also likely to indicate retention in the streambed sediments. Further, detailed experiments combining

particles, sediment and hydrodynamical characterization are needed to achieve generalizable information on MPs transport and retention.

3.4. Opportunities and Limitations

Using the analytical methods introduced in this work, we can quantitatively study the transport of fluorescent MPs in both surface water and hyporheic sediments in an experimental flume. Mass fluxes for MPs in and out of the control volume were measured using portable fluorometers. For a single bedform, the FIS was successfully used to quantify the migration and re-distribution of MPs (a) in the surface flow, (b) at the streambed interface and (c) in the streambed sediments. By applying the FIS, for the first time the advective transfer of pore-scale MPs from the surface flow into the streambed could be directly observed. This experimental setup can be used to achieve an improved quantitative understanding of the basic mechanisms governing MPs transport and retention in riverine environments. The setup can be used for a large variety of potential application scenarios, such as experiments (a) to investigate how sedimentation and erosion cycles in fluvial systems control MPs abundances in stream flow and streambed sediments, (b) to quantitatively understand retention mechanisms in streambed sediments by using different porous media (e.g., sand, clay, iron-oxides) and non-uniform geochemical conditions (pH, ionic strength), (c) to understand dynamics of re-suspension of MPs during high-flow events which are reported as hot moments of MPs contamination in rivers and streams (Hurley et al., 2018) and (d) to investigate how interactions with biota (uptake and excretion or biofilm formation) is affecting hydrodynamic properties of MPs in rivers and streams.

The methods facilitate an analysis of rapidly changing MPs concentrations, with a maximum sampling frequency of 0.5 Hz using the Fluorometers and 8 Hz using the Fluorescence-Imaging-System. Surface water concentrations of both techniques matched after the initial breakthrough. Due to particle adhesion and mixing in the tubing, the flow to the Fluorometers represents a potential source of error. A significant advantage of the FIS is its non-invasive nature, avoiding disturbances of the hydrodynamic conditions in the flume. However, optical access to a longitudinal flow section is required and therefore, the method is only suitable for a flume with a transparent glass or plexiglass window. In addition, the FIS visualizes subsurface flow only at the sediment-glass interface where the surface flow is influenced by the glass boundary and the subsurface flow by a locally higher porosity (Roozbahani et al., 2014), possibly leading to preferential flow paths. This effect is important for MPs larger than the average pore size of the sediment but was likely to be negligible in our experiment. Indeed, the identified subsurface flow pattern, infiltration at the troughs and exfiltration at the crests, was similar to direct measurements of dissolved tracers in hyporheic sediments (Precht & Huettel, 2004).

The methods can only be applied in combination with fluorescent MPs, which enable a clear separation of MPs from other, non-fluorescent suspended particles. While requiring the additional step of fluorescent staining, cross-contamination with ambient MP and other natural particles is negligible. The measurement also requires stability of the fluorescent signal over time, otherwise decreasing signal strength may be interpreted as lower particle abundances. This can be problematic since fluorescent tracers are known to leach and to degrade after light exposure (Gombert et al., 2017). Therefore, reference measurements with MPs samples stored in the same laboratory should be performed alongside long-term experiments. Quantification with fluorometers worked best for small, pore scale MPs (1 μm), since particle distribution in the flow and in the measurement cell is more homogeneous. With increasing particle size (10 μm), the signal intensity fluctuated which is possibly caused by the irregular passing of particles in the flow cell. Larger and denser particles may restrict the usability of a fluorescence spectrometer if they settle in the cuvette during measurement.

Additionally, we note that by measuring particle concentration in the flume, we track the movement of particle clouds rather than individual particles. For example, 1 μm particles cannot be resolved individually with a pixel size of 6.5 μm. At the detection limit of the fluorometers, a mass concentration of 0.5 μg/L corresponds to abundances of $\approx 10^6$ particles/L. Data on environmentally relevant concentrations of pore-scale MPs are not known due to analytical detection limits, but studies indicate an increasing abundance of smaller particles (Frei et al., 2019; Poulain et al., 2019). Since particle-particle interaction was avoided by tenside coating and an impact of the particles on the hydrodynamics can be neglected due to the small volumetric concentration, the transport mechanisms as observed at the laboratory scale should be transferable to real fluvial systems.

4. Conclusion

To our knowledge, the methods presented here are the first published that are able to quantitatively measure MPs transport and retention in a fluvial model environment by simultaneously tracking particle migration in surface flow and in streambed sediments. Using optical techniques, infiltration of MPs into the hyporheic zone was directly visualized and spatiotemporally resolved, which is necessary to gain insights into the mechanisms controlling MP mobility in rivers and streams. The presented method can be used for a combination of pore-scale MPs particles, sediments and bedform structures. This allows for an investigation of various scenarios of MPs transport in fluvial systems, which likely depends on relative particle size, shape, and polymer. Further experiments are necessary to clarify whether infiltrating particles are immobilized permanently in the riverbed sediment, or rather constantly migrate in a dynamic equilibrium. In the future, it will be possible to analyze how small-scale topographical features such as bedforms as well as moving bedforms influence the advective transfer, sedimentation and remobilization of MPs in fluvial systems.

We hope that our experimental setup will help other researchers to implement their own experimental system to investigate the fate of MPs in fluvial ecosystems. Although the presented methods are only partially suitable for application in real stream environments (application of portable fluorometers), we strongly believe that they are very useful to better understand and investigate the fundamental transport and retention mechanisms of MPs in rivers and streams.

Conflict of Interest

The authors declare no conflicts of interest relevant to this study.

Data Availability Statement

The data sets used and analyzed during the current study, as well as the developed MATLAB scripts are published in Zenodo (Boos et al., 2021): https://doi.org/10.5281/zenodo.5706440.

Acknowledgments
This study was funded by the Deutsche Forschungsgemeinschaft (DFG, German Research Foundation) – Project Number 391977956 – SFB 1357. The authors would like to thank the two reviewers for their valuable suggestions to improve the manuscript.

References

Andrady, A. L. (2011). Microplastics in the marine environment. *Marine Pollution Bulletin*, *62*(8), 1596–1605. https://doi.org/10.1016/j.marpolbul.2011.05.030

Baldwin, A. K., Corsi, S. R., & Mason, S. A. (2016). Plastic Debris in 29 Great Lakes Tributaries: Relations to watershed attributes and hydrology. *Environmental Science & Technology*, *50*(19), 10377–10385. https://doi.org/10.1021/acs.est.6b02917

Boos, J.-P., Gilfedder, B. S., & Frei, S. (2021). Data and code for the publication "Tracking microplastics across the streambed interface: Using laser-induced-fluorescence to quantitatively analyze microplastic transport in an experimental flume". https://doi.org/10.5281/zenodo.5706440

Carbery, M., O'Connor, W., & Palanisami, T. (2018). Trophic transfer of microplastics and mixed contaminants in the marine food web and implications for human health. *Environment International*, *115*, 400–409. https://doi.org/10.1016/j.envint.2018.03.007

Cook, S., Chan, H.-L., Abolfathi, S., Bending, G. D., Schäfer, H., & Pearson, J. M. (2020). Longitudinal dispersion of microplastics in aquatic flows using fluorometric techniques. *Water Research*, *170*, 115337. https://doi.org/10.1016/j.watres.2019.115337

Drummond, J. D., Nel, H. A., Packman, A. I., & Krause, S. (2020). Significance of hyporheic exchange for predicting microplastic fate in rivers. *Environmental Science and Technology Letters*, *7*(10), 727–732. https://doi.org/10.1021/acs.estlett.0c00595

Elliott, A. H., & Brooks, N. H. (1997). Transfer of nonsorbing solutes to a streambed with bed forms. *Laboratory experiments*, *33*(1), 137–151. https://doi.org/10.1029/96WR02783

Engelund, F., & Fredsoe, J. (1982). Sediment ripples and dunes. *Annual Review of Fluid Mechanics*, *14*(1), 13–37. https://doi.org/10.1146/annurev.fl.14.010182.000305

Fox, A., Boano, F., & Arnon, S. (2014). Impact of losing and gaining streamflow conditions on hyporheic exchange fluxes induced by dune-shaped bed forms. *Water Resources Research*, *50*(3), 1895–1907. https://doi.org/10.1002/2013WR014668

Free, C. M., Jensen, O. P., Mason, S. A., Eriksen, M., Williamson, N. J., & Boldgiv, B. (2014). High-levels of microplastic pollution in a large, remote, mountain lake. *Marine Pollution Bulletin*, *85*(1), 156–163. https://doi.org/10.1016/j.marpolbul.2014.06.001

Frei, S., Piehl, S., Gilfedder, B. S., Löder, M. G. J., Krutzke, J., Wilhelm, L., & Laforsch, C. (2019). Occurence of microplastics in the hyporheic zone of rivers. *Scientific Reports*, *9*(1), 15256. https://doi.org/10.1038/s41598-019-51741-5

Frias, J. P. G. L., & Nash, R. (2019). Microplastics: Finding a consensus on the definition. *Marine Pollution Bulletin*, *138*, 145–147. https://doi.org/10.1016/j.marpolbul.2018.11.022

Goeppert, N., & Goldscheider, N. (2021). Experimental field evidence for transport of microplastic tracers over large distances in an alluvial aquifer. *Journal of Hazardous Materials*, *408*, 124844. https://doi.org/10.1016/j.jhazmat.2020.124844

Goeppert, N., & Hoetzl, H. (2010). Precise method for continuous measurement of fluorescent microspheres during flow. *Hydrogeology Journal*, *18*(2), 317–324. https://doi.org/10.1007/s10040-009-0517-0

Gombert, P., Biaudet, H., Sèze, R. de, Pandard, P., & Carré, J. (2017). Toxicity of fluorescent tracers and their degradation byproducts. *International Journal of Speleology*, *46*(1), 23–31. https://doi.org/10.5038/1827-806X.46.1.1995

Haberstroh, C. J., Arias, M. E., Yin, Z., & Wang, M. C. (2020). Effects of hydrodynamics on the cross-sectional distribution and transport of plastic in an urban coastal river. *Water Environment Research*, *93*(2), 186–200. https://doi.org/10.1002/wer.1386

Haque, M. I., & Mahmood, K. (1985). Geometry of ripples and dunes. *Journal of Hydraulic Engineering*, *111*(1), 48–63. https://doi.org/10.1061/(ASCE)0733-9429(1985)111:1(48)

Harvey, J. W., Drummond, J. D., Martin, R. L., McPhillips, L. E., Packman, A. I., Jerolmack, D. J., et al. (2012). Hydrogeomorphology of the hyporheic zone: Stream solute and fine particle interactions with a dynamic streambed. *Journal of Geophysical Research*, *117*(G4). https://doi.org/10.1029/2012JG002043

Hoellein, T. J., Shogren, A. J., Tank, J. L., Risteca, P., & Kelly, J. J. (2019). Microplastic deposition velocity in streams follows patterns for naturally occurring allochthonous particles. *Scientific Reports*, *9*(1), 3740. https://doi.org/10.1038/s41598-019-40126-3

Horton, A. A., & Dixon, S. J. (2018). Microplastics: An introduction to environmental transport processes. *Wiley Interdisciplinary Reviews: Water*, *5*(2), e1268. https://doi.org/10.1002/wat2.1268

Hurley, R., Woodward, J., & Rothwell, J. J. (2018). Microplastic contamination of river beds significantly reduced by catchment-wide flooding. *Nature Geoscience*, *11*(4), 251–257. https://doi.org/10.1038/s41561-018-0080-1

Jemec, A., Horvat, P., Kunej, U., Bele, M., & Kržan, A. (2016). Uptake and effects of microplastic textile fibers on freshwater crustacean Daphnia magna. *Environmental Pollution*, *219*, 201–209. https://doi.org/10.1016/j.envpol.2016.10.037

Kowalski, N., Reichardt, A. M., & Waniek, J. J. (2016). Sinking rates of microplastics and potential implications of their alteration by physical, biological, and chemical factors. *Marine Pollution Bulletin*, *109*(1), 310–319. https://doi.org/10.1016/j.marpolbul.2016.05.064

Law, K. L., Morét-Ferguson, S., Maximenko, N. A., & Proskurowski, G. (2010). Plastic Accumulation in the North Atlantic Subtropical Gyre. *Science*, *329*. https://doi.org/10.1126/science.1192321o

Li, C., Busquets, R., & Campos, L. C. (2020). Assessment of microplastics in freshwater systems: A review. *Science of the Total Environment*, *707*, 135578. https://doi.org/10.1016/j.scitotenv.2019.135578

Los Santos, C. B., Krång, A.-S., & Infantes, E. (2021). Microplastic retention by marine vegetated canopies: Simulations with seagrass meadows in a hydraulic flume. *Environmental Pollution*, *269*, 116050. https://doi.org/10.1016/j.envpol.2020.116050

Lu, T., Gilfedder, B. S., Peng, H., Niu, G., & Frei, S. (2021). Effects of clay minerals on the transport of nanoplastics through water-saturated porous media. *Science of the Total Environment*, *796*, 148982. https://doi.org/10.1016/j.scitotenv.2021.148982

Lu, T., Gilfedder, B. S., Peng, H., Peiffer, S., Papastavrou, G., Ottermann, K., & Frei, S. (2021). Relevance of iron oxyhydroxide and pore water chemistry on the mobility of nanoplastic particles in water-saturated porous media environments. *Water, Air, & Soil Pollution*, *232*(5). https://doi.org/10.1007/s11270-021-05125-z

Mani, T., Primpke, S., Lorenz, C., Gerdts, G., & Burkhardt-Holm, P. (2019). Microplastic pollution in benthic midstream sediments of the Rhine River. *Environmental Science & Technology*, *53*(10), 6053–6062. https://doi.org/10.1021/acs.est.9b01363

Meijer, L. J. J., van Emmerik, T., van der Ent, R., Schmidt, C., & Lebreton, L. (2021). More than 1000 rivers account for 80% of global riverine plastic emissions into the ocean. *Science Advances*, *7*(18). https://doi.org/10.1126/sciadv.aaz5803

Nizzetto, L., Bussi, G., Futter, M. N., Butterfield, D., & Whitehead, P. G. (2016). A theoretical assessment of microplastic transport in river catchments and their retention by soils and river sediments. *Environmental Science. Processes & Impacts*, *18*(8), 1050–1059. https://doi.org/10.1039/c6em00206d

Ockelford, A., Cundy, A., & Ebdon, J. E. (2020). Storm response of fluvial sedimentary microplastics. *Scientific Reports*, *10*(1), 1865. https://doi.org/10.1038/s41598-020-58765-2

Peeken, I., Primpke, S., Beyer, B., Gütermann, J., Katlein, C., Krumpen, T., et al. (2018). Arctic sea ice is an important temporal sink and means of transport for microplastic. *Nature Communications*, *9*(1), 1505. https://doi.org/10.1038/s41467-018-03825-5

Poulain, M., Mercier, M. J., Brach, L., Martignac, M., Routaboul, C., Perez, E., et al. (2019). Small microplastics as a main contributor to plastic mass balance in the North Atlantic subtropical gyre. *Environmental Science & Technology*, *53*(3), 1157–1164. https://doi.org/10.1021/acs.est.8b05458

Precht, E., & Huettel, M. (2004). Rapid wave-driven advective pore water exchange in a permeable coastal sediment. *Journal of Sea Research*, *51*(2), 93–107. https://doi.org/10.1016/j.seares.2003.07.003

Roozbahani, M. M., Graham-Brady, L., & Frost, J. D. (2014). Mechanical trapping of fine particles in a medium of mono-sized randomly packed spheres. *International Journal for Numerical and Analytical Methods in Geomechanics*, *38*(17), 1776–1791. https://doi.org/10.1002/nag.2276

Schnegg, P.-A. (2002). *An inexpensive field fluorometer for hydrogeological tracer tests with three tracers and turbidity measurement* (pp. 1484–1488). Groundwater and Human Development.

Shahul Hamid, F., Bhatti, M. S., Anuar, N., Anuar, N., Mohan, P., & Periathamby, A. (2018). Worldwide distribution and abundance of microplastic: How dire is the situation? *Waste Management & Research*, *36*(10), 873–897. https://doi.org/10.1177/0734242X18785730

Skalska, K., Ockelford, A., Ebdon, J. E., & Cundy, A. B. (2020). Riverine microplastics: Behaviour, spatio-temporal variability, and recommendations for standardised sampling and monitoring. *Journal of Water Process Engineering*, *38*, 101600. https://doi.org/10.1016/j.jwpe.2020.101600

The MathWorks Inc. (2019). *MATLAB and image processing toolbox R2019b*. Massachusetts: Natick.

Tibbetts, J., Krause, S., Lynch, I., & Sambrook Smith, G. (2018). Abundance, distribution, and drivers of microplastic contamination in urban river environments. *Water*, *10*(11), 1597. https://doi.org/10.3390/w10111597

Waldschläger, K., & Schüttrumpf, H. (2019a). Effects of particle properties on the settling and rise velocities of microplastics in freshwater under laboratory conditions. *Environmental Science & Technology*, *53*(4), 1958–1966. https://doi.org/10.1021/acs.est.8b06794

Waldschläger, K., & Schüttrumpf, H. (2019b). Erosion behavior of different microplastic particles in comparison to natural sediments. *Environmental Science & Technology*, *53*(22), 13219–13227. https://doi.org/10.1021/acs.est.9b05394

Waldschläger, K., & Schüttrumpf, H. (2020). Infiltration behavior of microplastic particles with different densities, sizes, and shapes-from glass spheres to natural sediments. *Environmental Science & Technology*, *54*(15), 9366–9373. https://doi.org/10.1021/acs.est.0c01722

Watkins, L., McGrattan, S., Sullivan, P. J., & Walter, M. T. (2019). The effect of dams on river transport of microplastic pollution. *Science of the Total Environment*, *664*, 834–840. https://doi.org/10.1016/j.scitotenv.2019.02.028

Windsor, F. M., Tilley, R. M., Tyler, C. R., & Ormerod, S. J. (2019). Microplastic ingestion by riverine macroinvertebrates. *Science of the Total Environment*, *646*, 68–74. https://doi.org/10.1016/j.scitotenv.2018.07.271

Woodall, L. C., Sanchez-Vidal, A., Canals, M., Paterson, G. L. J., Coppock, R., Sleight, V., et al. (2014). The deep sea is a major sink for microplastic debris. *Royal Society Open Science*, *1*(4), 140317. https://doi.org/10.1098/rsos.140317